er nictitating membrane potentials in the EOG. REM sleep was defined by low voltage (< 50 μV), fast (> 10 cycles per second) EEG activity, eye movements occurring singly and in bursts, and tonic EMG activity equal or lower in amplitude to that of preceding SWS. Transitions from SWS to wakefulness were invariably associated with increased EMG activity.

There were no statistically significant changes in total sleep time throughout the fast (Table 1). However, the nocturnal minimum T_s was lower in the two doves that slept the most (30° and 32°C) than in the two that slept the least (35° and 34°C). Regardless of how much they slept, all four doves spent less of their total sleep time in REM sleep on the last fasting night than on baseline nights ($P < .05$, Table 1).

There are striking similarities between these sleep and T_b patterns of doves and those of mammals during torpor (*1–3*). Like ground squirrels and pocket mice, doves enter shallow torpor while asleep, displaying reduced amounts of REM sleep as T_b falls (*10*). Cooling the hypothalamus of kangaroo rats also reduces REM sleep (*11*). Since thermoregulatory processes are switched off during REM sleep (*12*), T_b related reductions in REM sleep may be a kind of homeostatic adjustment bringing about almost continuous regulation of T_b during torpor.

In the marmot, SWS was also associated with declines in brain temperature during entrance into hibernation (*4*). Although intermittent periods of wakefulness tended to be longer and behaviorally more active than in the ground squirrel (*2*), extended active episodes were accompanied by a decrease in the rate of decline of brain temperature or even an increase [figure 3 in (*4*)], as in squirrels. Episodes of intermittent wakefulness were shorter during entrance into torpor in the dove than in mammals (*2, 4*) and did not affect the course of the decline in T_b.

The decreased EEG amplitude associated with the decline in T_b points to the temperature dependence of neural activity. Similar EEG attentuation occurs in reptiles exposed to low T_a's (*13*) and in hypothermic nonhibernating mammals (*14*). In other respects, the EEG characteristics of SWS, REM sleep, and wakefulness during shallow torpor were essentially unaltered.

The doves always entered shallow torpor at times corresponding to their usual sleep-associated circadian decrease in T_b immediately following the onset of darkness (Fig. 1), unlike ground squirrels and pocket mice which sometimes enter torpor at times remote from their normal circadian decreases in T_b (*1, 3*). However, shallow torpor and hibernation are polyphyletic phenomena (*15*) and their temporal occurrence, duration, and depth are linked with several factors, such as T_a, body size, food availability, and amount of adipose tissue. Nevertheless, the correlation between shallow torpor and sleep in doves provides support for the suggestion that SWS and torpor in birds and mammals are homologous processes varying in depth along a continuum of decreasing T_b and metabolism. The ubiquity of drops of 1° or 2°C in T_b during sleep, with further drops into shallow torpor being contingent on negative energy balances, is to be expected if the positive curvilinear relation between metabolic rate and body-T_a differential shown for bats at T_a's below thermoneutrality (*16*) applies to most endotherms. Thus initial drops in T_b of 1° or 2°C during sleep yield greater energy savings (and would, therefore, be under greater evolutionary selective pressure) than subsequent reductions in T_b of equal magnitude during shallow torpor.

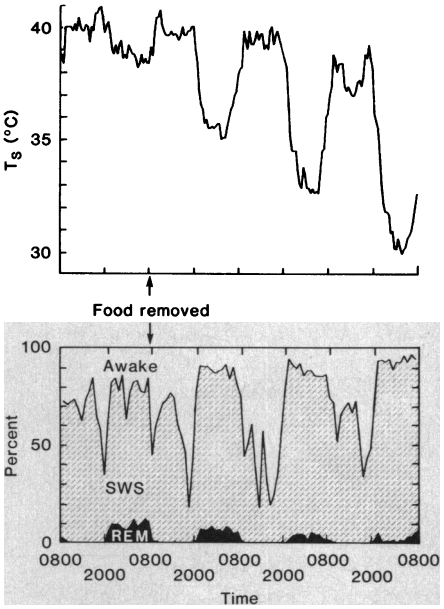

Fig. 1. Skin temperature (T_s) and percentages of time awake and in slow-wave sleep (*SWS*) or rapid-eye-movement sleep (*REM*) for a dove before and throughout a 3-day fast. Note the 9° drop in T_s and virtual disappearance of REM sleep during the last 24 hours of the fast.

LARRY E. WALKER
JAMES M. WALKER
JOSEPH W. PALCA
RALPH J. BERGER

Department of Biology, University of California, Santa Cruz 95064

References and Notes

1. J. M. Walker and R. J. Berger. *Prog. Brain Res.* **53**, 255 (1980); R. J. Berger, *Biol. Psychol.*, in press.
2. J. M. Walker, S. F. Glotzbach, R. J. Berger, H. C. Heller, *Am. J. Physiol.* **233**, R213 (1977).
3. J. M. Walker, A. Garber, R. J. Berger, H. C. Heller, *Science* **204**, 1098 (1979).
4. V. M. Miller and F. E. South, *Physiol. Behav.* **27**, 989 (1981).
5. S. F. Glotzbach and H. C. Heller, *Science* **194**, 537 (1976); G. L. Florant, B. Turner, H. C. Heller, *Am. J. Physiol.* **235**, R82 (1978).
6. R. C. Lasiewski, *Physiol. Zool.* **36**, 122 (1963).
7. E. D. Ketterson and J. R. King, *ibid.* **50**, 115 (1977).
8. R. C. MacMillen and C. H. Trost, *Comp. Biochem. Physiol.* **23**, 243 (1967).
9. J. M. Walker and R. J. Berger, *Behav. Biol.* **7**, 195 (1972).
10. J. M. Walker, E. H. Haskell, R. J. Berger, H. C. Heller, *Experientia* **37**, 726 (1981).
11. S. Sakaguchi, S. F. Glotzbach, H. C. Heller, *Am. J. Physiol.* **237**, R80 (1979).
12. P. L. Parmeggiani and C. Rabini, *Arch. Ital. Biol.* **108**, 369 (1970); H. C. Heller and S. F. Glotzbach, *Int. Rev. Physiol.* **15**, 147 (1977); P. L. Parmeggiani, in *Physiology in Sleep*, J. Orem and D. Barnes, Eds. (Academic Press, New York, 1980), p. 97.
13. J. M. Walker and R. J. Berger, *Brain Behav. Evol.* **8**, 453 (1973).
14. J. ten Cate, G. P. M. Horsten, L. J. Koopman, *Electroencephalogr. Clin. Neurophysiol.* **1**, 231 (1949); W. P. Koella and H. M. Ballin, *Arch. Int. Physiol.* **62**, 369 (1954); J. W. Scott, *Electroencephalogr. Clin. Neurophysiol.* **7**, 466 (1955).
15. G. A. Bartholomew, in *Hibernation and Hypothermia, Perspectives and Challenges*, F. E. South, J. P. Hannon, J. R. Willis, E. T. Pengelley, N. R. Alpert, Eds. (Elsevier, Amsterdam, 1972), p. 663; C. P. Lyman, in *Strategies in Cold: Natural Torpidity and Thermogenesis*, L. C. H. Wang and J. W. Hudson, Eds. (Academic Press, New York, 1978), p. 9.
16. E. H. Studier, *Comp. Biochem. Physiol.* **70A**, 537 (1981).

17. Supported by NIH grant GM23694 and a University of California, Santa Cruz, faculty research grant to R.J.B.

20 October 1982; revised 14 March 1983

Circumglobal Transport of the El Chichón Volcanic Dust Cloud

Abstract. *The stratospheric dust cloud from the 4 April 1982 eruption of El Chichón volcano in southern Mexico was observed to travel completely around the world in a 3-week period. Images from satellites operated by the National Oceanic and Atmospheric Administration were used to prepare daily maps of the location of the volcanic dust cloud, which is the largest and longest-lasting one so far observed with satellite imagery.*

On 4 April 1982, after one eruption on 28 March and two on 3 April, El Chichón volcano in southern Mexico erupted violently, sending a dense cloud of dust into the stratosphere. Lidar observations on 10 and 11 April from Hawaii, made as the densest part of the cloud passed over, showed that the highest concentration of dust was at an altitude of approximately 26 km, well above the tropopause, which

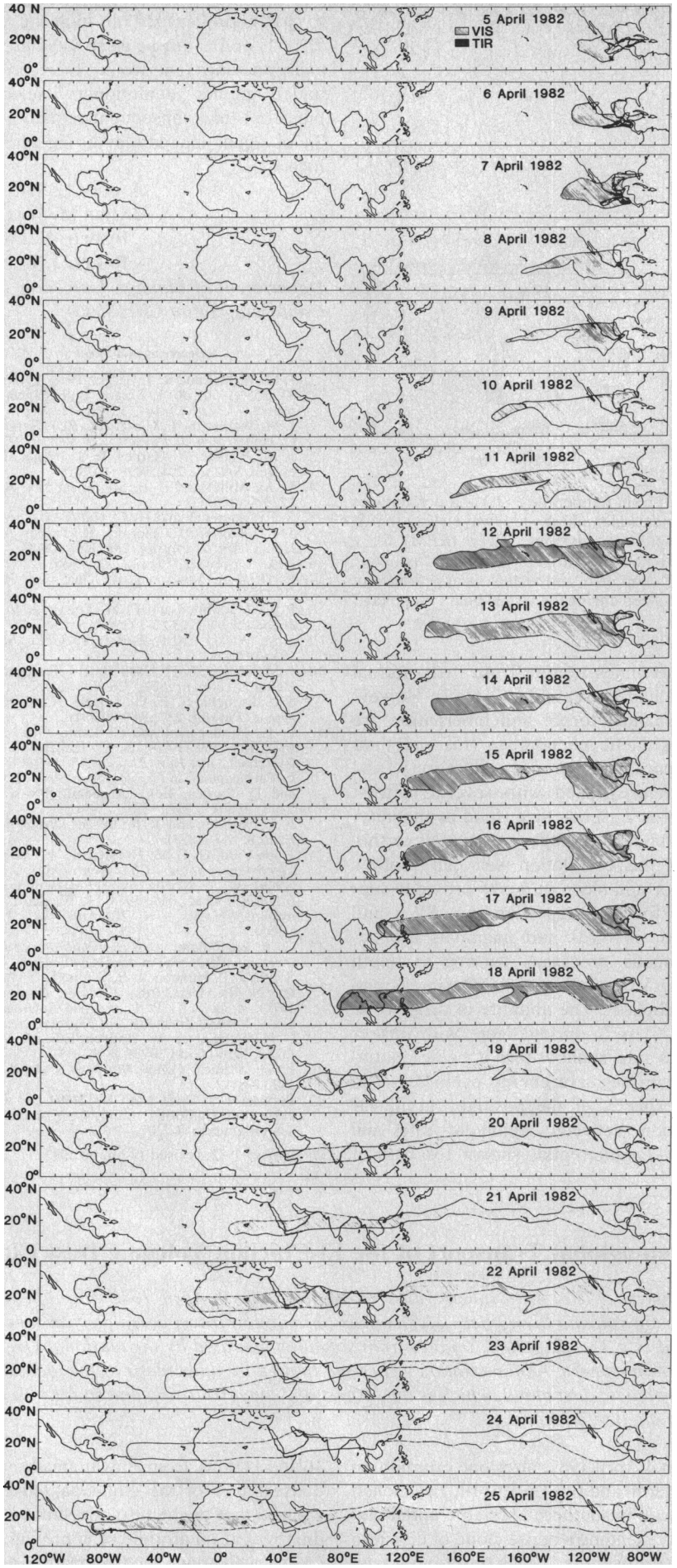

was at 16 km. In the past 2 years we have observed volcanic dust clouds from the eruptions of Mount St. Helens (*1*), Alaid (U.S.S.R.), and Galunggung (Indonesia) with satellite imagery and found that the dust was undetectable after only 2 or 3 days. That El Chichón put much more dust into the stratosphere is indicated by the fact that we could detect its dust cloud for at least 1 month after the eruption.

Figure 1 shows maps of the location of the dust cloud for each day after the eruption until 25 April, when the cloud had circled the globe. After this time, although the dust was still visible on some images, it was very difficult to detect the edge of the dust cloud. For longitudes in the Western Hemisphere west of the volcano, we used imagery from the geostationary GOES-E and GOES-W satellites, which is received every 30 minutes. These portions of the maps are plotted at 0000 Greenwich mean time (GMT). For the Eastern Hemisphere, and westward across the Atlantic, we used images from the polar-orbiting NOAA-7 satellite, which produces one daytime image at approximately 1500 local time at the latitude of the dust (18°N). These portions of the maps are plotted to correspond to the images and thus are for 0300 GMT at longitude 180°, 0400 GMT at 165°E, and so on up to 2000 GMT at 75°W. We could detect the dust for only a few days after the eruption with GOES thermal infrared imagery, and this cloud boundary is also plotted on the maps. The sensors on the satellites detect reflected solar radiation in the wavelength bands 0.58 to 0.68 μm (NOAA-7) and 0.55 to 0.75 μm (GOES), and thermal infrared in the wavelength band 10.5 to 12.5 μm (GOES).

Figure 2 is an example of the satellite pictures we used. We detected the dust in the pictures by observing areas of gray, as opposed to black, over oceans (*A* in Fig. 2), or areas where the surface features or clouds appeared blurry (*B* in Fig. 2). In some cases it was impossible to detect the dust because of "sun glint"—reflection of sunlight off the ocean waves, giving a gray appearance similar to that of the dust (*C* in Fig. 2). It was also impossible to detect the dust in regions of overcast featureless cloud

Fig. 1. Location of the dust cloud from the El Chichón eruption as observed with visible (*VIS*) and thermal infrared (*TIR*) imagery. Portions of the cloud to the right of 180° are plotted at 0000 GMT. Portions to the left of 180° are plotted at 1500 local time. Dash-dot lines indicate difficulties in observing the exact location of the edge of the cloud.

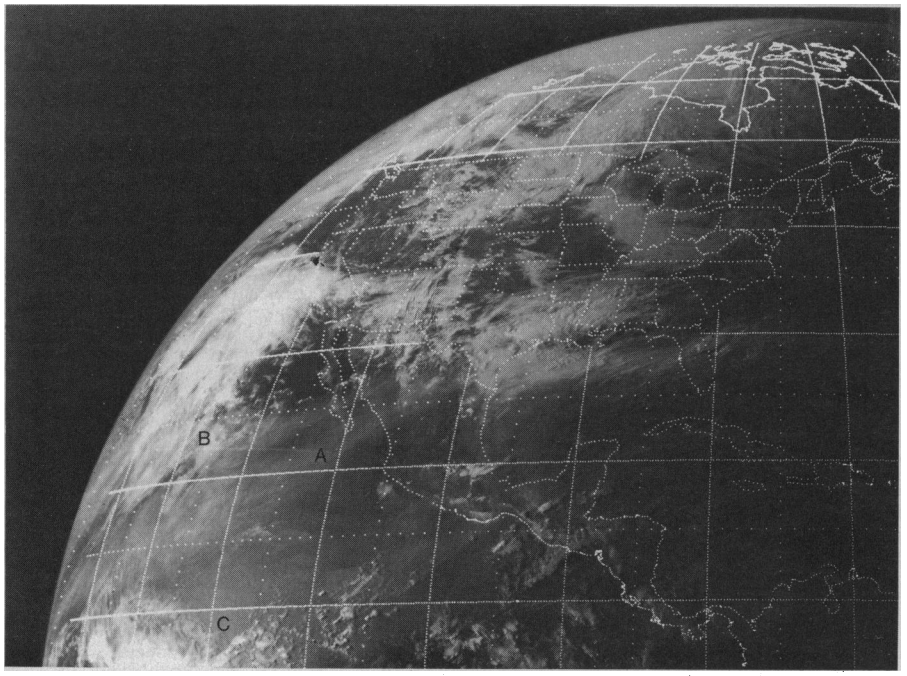

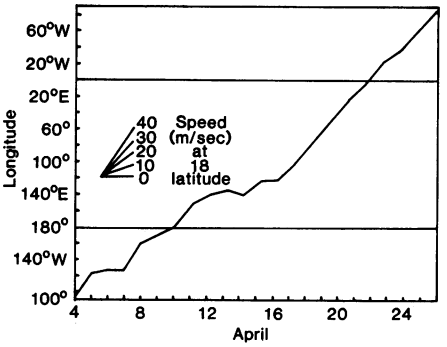

Fig. 2 (left). GOES-E visible image taken at 2300 GMT on 9 April 1982, illustrating the gray appearance of the dust over the ocean (*A*), the blurring of clouds (*B*), and sun glint (*C*). Fig. 3 (right). Longitude of the leading edge of the dust as a function of time.

decks. The regions where the edge of the dust cloud was undetectable are indicated by dash-dot lines in Fig. 1.

It can be seen in Fig. 1 that the leading edge of the dust moved toward the west during the entire period. Winds at 30 mbar, at an altitude of approximately 24 km, had just begun to blow from the east at the time of the eruption as the circumpolar stratospheric circulation began its shift into the summer pattern of easterlies. The quasi-biennial oscillation was at its maximum easterly phase, so that stratospheric winds over the region between 10°N and 10°S were at approximately 25 m/sec from the east. The dust cloud appears to stretch out in longitude during the period but exhibits very little latitudinal motion, remaining in the band from 10°N to 30°N.

Figure 3 shows the longitude of the leading edge of the dust as a function of time. Also plotted are lines with slopes representing different speeds at the latitude of the dust. The dust moved more slowly during the first 12 days after the 4 April eruption and then speeded up as the summer stratospheric circulation established itself. The average speed during the entire period was 22 m/sec. We attempted to compare the observed 30-mbar winds at the leading edge of the dust with the velocity of the dust itself, but found that in all but a few cases there were no wind observations near the dust edge. (For these few cases, the observed winds were in agreement with the observed transport speed of the dust.) Our observations of the transport of the dust thus provide a better measure of winds at this altitude and latitude than is available from the conventional radiosonde network.

The vertical and horizontal distribution of the dust depends on a number of factors. The source of the dust was a brief (several hours) injection at one point. Additional particles formed in situ from sulfur gases after the eruption. The stretching out of the dust cloud in longitude may be due to vertical wind shear, giving different transport velocities at different heights. This study, in combination with other observations of the dust, will allow us to better understand the nature and distribution of this immense dust cloud and to calculate its implications for the future climate.

ALAN ROBOCK
Department of Meteorology, University of Maryland, College Park 20742

MICHAEL MATSON
NOAA/National Environmental Satellite, Data, and Information Service, Suitland Professional Center, Washington, D.C. 20233

References and Notes

1. A. Robock and C. Mass, *Science* **216**, 628 (1982); C. Mass and A. Robock, *Mon. Weather Rev.* **110**, 614 (1982).
2. We thank K. Labitzke for supplying us with 30-mbar maps for April and E. King and J. Kline for drafting the figures. This research was supported by NSF grant ATM-7918125 and NOAA grant ATM-80-24881.

10 November 1982; revised 4 March 1983